Potential wettability alteration/IOR study for pre-salt carbonate by low salinity brines: from experiments to field scale simulation

Omid Karoussi[1,*], *Rex* M.S. Wat[2], *Claudio* De Lima[3], and *Lidiana* Ribeiro[3]

[1)] Equinor ASA, Stavanger, Norway, [2)] Equinor ASA, Trondheim, Norway, [3)] Equinor, Brazil

Abstract. Majority of carbonates reservoirs are known to be mixed to oil wet in terms of wettability. The wetting behaviour of these rocks becomes even more complicated due to the heterogeneous and complex, multimodal pore systems. To our knowledge, the Brazilian deep water pre-salt lacustrine carbonate reservoirs are a tailor-end and even more complex prolific rocks that have not been investigated under the same extent as other more conventional carbonates such as North Sea chalk or Middle East Limestone/Dolomite. They also coexist with an abnormally high salinity formation brine (TDS ~ 330k ppm) that introduces even more complexity to the nature of these reservoirs. When sea water (TDS ~ 35k ppm) is injected for pressure support, the wetting behaviour of the reservoir rock is greatly impacted due to the large salinity shift. In this study, a combined research project together with a commercial SCAL program for a pre-salt carbonate field were performed to investigate the effect of sea water injection on the improved oil recovery as well as the determination of relative permeability function under wettability alteration mechanism. Both spontaneous imbibition tests at elevated temperature and steady state relative permeability experiment at reservoir condition on actual reservoir core sample were conducted and the results are used as input to reservoir simulation studies.

1 Introduction

Wettability alteration to more water wet condition on reservoir rocks has been widely studied and introduced as the positive contributing mechanism to increase oil recovery since oil affinity to the rock is reduced and more oil can be produced. Katende and Sagala [1] provided a comprehensive summary, where the wettability alteration is addressed as the main mechanism for low salinity water flooding/injection (LSW) studies as IOR/EOR method. They also give an overview of successful and unsuccessful field applications of LSW-flooding as well.

With reference to Petrowiki [2] "*Low-salinity water flooding (LSW) is an EOR method that injects water containing low concentrations of soluble solids into a reservoir. Its potential of improving oil production has been proved through laboratory experiments. Unlike the conventional water flooding, low-salinity water flooding can change the wettability of the reservoir rock in order to increase oil recovery. It is usually used as tertiary oil recovery technology and has great potential for oilfield development*". This method was first investigated by Bernard [3] in late 60's to see how salinity of the injected water could affect the efficiency of oil recovery. Since then, LSW has extensively been studied by various researcher across the world under two major themes of rock/fluid and fluid/fluid interactions mainly on sandstones as well summarized by Katende and Sagala [1].

Another comprehensive research by Nande and Patwardhan [4], summarizes all LSW mechanisms, performance studies and field applications particularly on carbonates rocks. They concluded that due to the heterogeneous and complex, multimodal pore systems and chemically active nature of these rocks compared to sandstone, LSW-flooding mechanism and implication in carbonates have not yet been completely understood, hence various mechanisms have been proposed by different researchers for IOR/EOR studies. Derkani et al. [5] and Hao et al. [6] reviewed LSW-flooding mechanisms by looking at rock-fluid interactions, whereas other researchers like Mokhtari et al. [7] and Rostami et al. [8] investigated fluid/fluid interaction. In common, they demonstrated that there is potential to improve oil recovery in carbonates by LSW flooding. They also indicated that due the complexity of both LSW flooding mechanisms and the nature of carbonate rocks, it is essential to investigate the rock/fluid and fluid/fluid interactions in more detail. The former was mainly addressed by wettability alteration, surface charges, fine migration and mineral composition of the rock and the latter was studied under oil/brine compositions, changes in interfacial tension (IFT) and pH due to the dissolution of polar components of oil to brine and/or dispersion of brine in oil phase at the interface.

Mahani et al. [9] showed that limestone rock became less oil-wet when diluted sea water were used. Recently, Wang et al. [10] and Mahmoodi et al. [11] also investigated the effect of salinity on wettability alteration

[*] Corresponding author: omkar@equinor.com

hence, improved oil mobilization in subsurface reservoirs by using Engineered Water Flood (EWF) or Modified Salinity Water (MSW) flooding, respectively. Mahmoodi et al. [11] studied the positive effect of sulphate removal (i.e. desulphation) as one way to modify seawater salinity and observed improved oil recovery in a brown field. In a different approach, Bordeaux-Rego et al [12] performed core flood modelling of pre-salt carbonate using Corey correlation as well as contact angle measurements for different brine. They reported a reduction in the measured contact angle as indicator for wettability alteration, for sea water system with salinity of around 50000 ppm as reference fluid followed by engineered water system (i.e. low salinity sea water down to 9000 ppm in salinity and no NaCl in brine).

Over the last decade, giant hydrocarbon reservoirs were discovered in Aptian age carbonates in Santos and Campos basins located offshore Brazil as illustrated by Sartorato et al [13] in Figure 1.

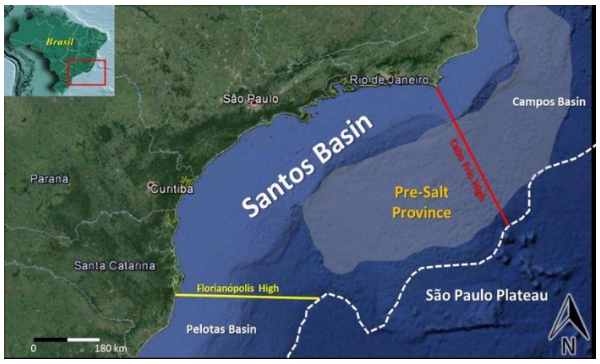

Fig.1. Location of the Santos and Campos basin offshore Brazil (after Sartorato et al [13]).

Figure 2 shows seal peels (i.e. preserved core intervals) of a pre-salt carbonate reservoir possessing lithology of dolomitic limestone on the left, and silicified carbonate and argillaceous carbonate on the right.

Fig. 2. Pre-salt carbonate (dolomitic-Limestone on the left, and silicified carbonate and argillaceous carbonate on the right).

In this study we have investigated the effects of desulphated sea water, mimicking LSW (i.e due to one order of magnitude difference between salinity of FW and DSSW), on oil recovery under spontaneous imbibition as well as steady state relative permeability measurements. The results were used to establish the relative permeability saturation functions as input to reservoir simulation studies aiming to quantify the oil recovery due to wettability alteration.

2 Experimental work and conditions

The core plugs used in this study were drilled from the preserved cores (4" in diameter) taken from wells drilled in pre-salt carbonate reservoir. The cores belonged to two different wells from a field located in Santos basin offshore Brazil (Figure 1). The spontaneous imbibition (SI) study at elevated temperature and steady state relative permeability (SS-K_r) measurement at reservoir condition were performed on selected plugs from the same rock type, mainly dolomitic limestone, where the analogous are shown in Figure 2.

2.1 Spontaneous imbibition test

Three core plugs (1.5" in diameter), as listed in Table 1, were used in SI tests. They were first conditioned to irreducible water saturation (S_{wi}) by centrifuge and aged with crude oil for 28 days at reservoir temperature. The tests were performed at atmospheric pressure and reservoir temperature, where the plugs were submerged into different brines sequentially. The corresponding fluid properties for each brine used are given in Table 2, where FW, DSSW, SSW and LSW stand for formation water, desulphated sea water, synthetic sea water and low salinity sea water, respectively.

Table 1. Plugs properties, SI test

Plug	L (cm)	D (cm)	Φ	kl (mD)
CE8-well A	4.78	3.81	0.134	134
CE22-well A	4.68	3.81	0.184	1598
CE28-well A	4.68	3.81	0.185	4364

L: length
D: diameter
Φ: Porosity
kl: Klingenberg corrected permeability

Table 2: Fluid properties, SI test

Fluid	μ (cP)	ρ (cc/g)	Salinity (k ppm)
FW	0.9955	1.1990	330
DSSW	0.4675	0.9978	30
SSW	0.5090	1.0028	35
LSW	0.7830	0.9975	1.4
Oil	4.937	0.8380	-

μ: Viscosity measured at 70ºC except LSW at 30ºC
ρ: Density measured at 70ºC except LSW at 30ºC

The amount of oil displaced by the imbibed water was recorded over time. As shown in Figure 3, when oil production ceased at equilibrium, the plugs were removed and placed in new pre-heated Amott cells prefilled with the next brine for the spontaneous imbibition to continue.

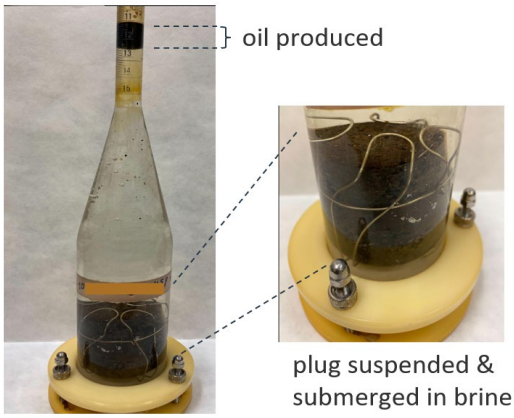

Fig. 3. Spontaneous Imbibition setup in an Amott cell.

2.2. Steady state relative permeability test

In this part of study, three SCAL plugs (1.5" in diameter) from the same rock type were allocated to SS-K_r measurements at reservoir conditions using either formation water (FW) or desulphated sea water (DSSW) as aqueous phase and recombined reservoir fluid as oil phase. The CT scan was done by Industrial CT with resolution of ~100 micron and the CT images for these three plugs are shown in Figure 4 indicating how heterogenous these samples are. The corresponding core plugs and fluid properties are summarized in Table 3 and Table 4, respectively.

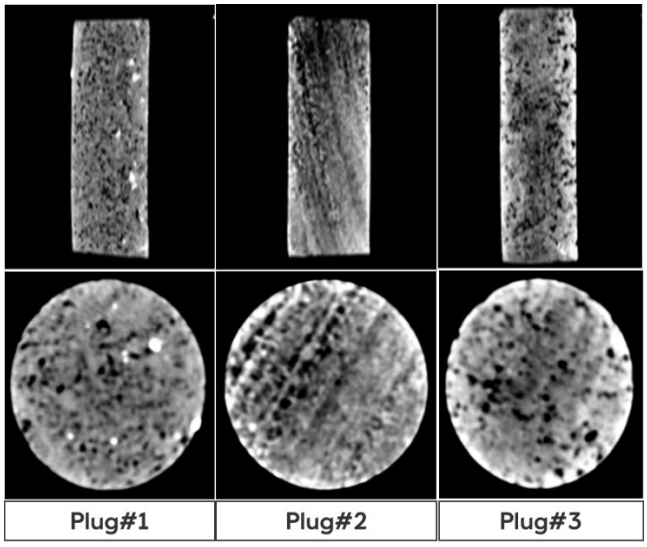

Fig. 4. CT images of SCAL plugs (longitudinal on top and cross section at bottom) used in SS-K_r test. The heterogeneity is clearly shown with big pores (pores/vugs in black), tight/cemented part in gray/white.

Table 3. SCAL plugs properties used in SS-Kr tests

Plug	L (cm)	D (cm)	Φ (frac.)	kl (mD)
Plug#1-well A	6.26	3.82	0.133	296.7
Plug#2-well A	6.00	3.80	0.196	22.9
Plug#3-well B	8.88	3.80	0.167	721.3

L: length
D: diameter
Φ: Porosity
kl: Klingenberg corrected permeability

Table 4: Fluid properties, SS-Kr test

Fulid	μ (cP)	ρ (cc/g)	Salinity (k ppm)
FW	$0.75^{(1)}/0.621^{(2)}$	$1.23^{(1)}/1.174^{(2)}$	330
DSSW	$0.309^{(1)}/0.314^{(2)}$	$1.026^{(1)}/0.995^{(2)}$	30
Oil	$0.42^{(1)}/0.332^{(2)}$	$0.638^{(1)}/0.611^{(2)}$	-

μ: Viscosity measured at reservoir condition
ρ: Density measured at reservoir condition
(1): Lab#1, Plug#1
(2): Lab#2, Plug#2, and Plug#3

The SS-K_r tests were run from the bottom of a vertically oriented core holder using a restored state horizontal core plug. The measurements were performed using a net confining pressure (NCP) of 150 bar. Doped brine (mutually equilibrated with recombined reservoir oil) was injected from the bottom of the plug sample for gravity stable injection of water and displacement of oil from the top. The experimental steps continued with a sequence of eight fraction flows of oil and water, where differential pressure, production data and the saturation profile under in-situ saturation monitoring (ISSM) by gamma ray were acquired. After the flooding test and relative permeability measurement were done for oil/FW system, the core plugs were cleaned through flooding and S_{wi} was re-established using FW by porous plate between 4-6 weeks and core were aged by live oil. Then, similar procedure was followed to perform oil/DSSW injection and relative permeability measurement, where the doped DSSW brine (mutually equilibrated with recombined reservoir oil is used as aqueous phase instead of FW.

A simple schematic of steady state relative permeability measurement set-up is illustrated in Figure 5. The experimental data was simulated (history matched) by Sendra software [14] as core flood simulator to generate relative permeability curves using LET correlations [15].

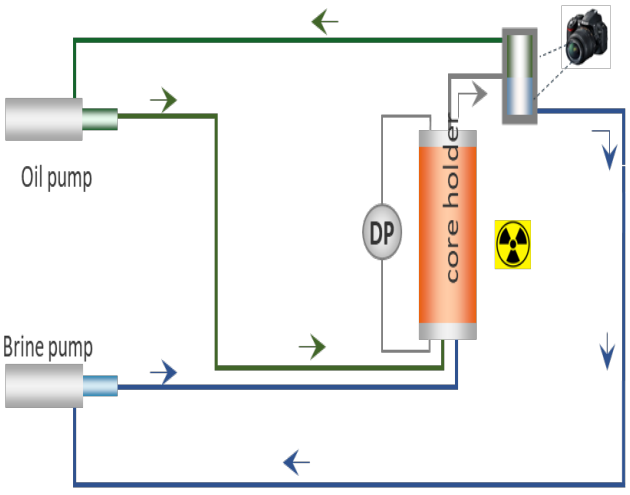

Fig. 5. Schematic of a typical steady state water-oil process; water and oil pump in re-circulation mode.

3 Results and Discussion

3.1 Spontaneous Imbibition results

The oil production profiles from the three tested core plugs are shown in Figure 6 indicating a clear incremental increase in the produced oil after switching to a different brine. In other words, the results obtained here for all three core plugs exhibit a systematic increase in additional oil production by changing the brine from FW to DSSW followed by Synthetic Sea Water (SSW) and Low salinity Sea Water (LSW). It is important to note that the first increase, when using FW, was primarily due to the conditioning step of the plugs when a high centrifuge speed of 6400 rpm was used to establish S_{wi}. In this case the in-situ brine was the same FW; whilst the subsequent increases were driven by the salinity effect as the plugs were sequentially transferred and submerged under different brine with different salinity. Due to low diffusion rate, an extended period of time was needed to reach equilibrium at each step. Overall, it took around 300 days to complete these tests.

In a recent study, Ramstad et al. [16], demonstrated the similar behaviour on increased oil production from pre-salt carbonate under SI test once the brine was switched from FW to SSW and DSSW. They also used high-resolution micro-CT to image the fluid distributions inside the core plugs once the brine was changed. Mahani et al. [9] showed that the limestone surfaces became less oil-wet by switching from FW to Sea Water (SW), and different desulphated Sea Water (dSW as abbreviation used in their paper). Mahmoodi et al. [11] reported a positive effect of sulphate removal (i.e. desulphation) as one way to modify seawater salinity and observed improved oil recovery in a brown field.

During the test, and before changing to the next brine, the core plug CE#08 was subjected to NMR scan with the aim to detect any changes of wettability inside the core. Unfortunately, these results were less conclusive.

It was also challenging to run SI at high temperature using Amott (glass) cell leading to occasional leakage with brine top up and air bubble evolution due to incomplete brine degasification. Toward the end with core plug CE22, it was the evolved gas bubbles forming 'gas-in-oil' emulsion that made reading the oil volume difficult. However, this 'gas-in-oil' emulsion was unstable. The decrease of 'observed' oil production was due to the collapse of such emulsion when reading was taken as also indicated in the Figure 6.

3.2 Steady State relative permeability results

As mentioned in section 2, three core plugs undergone steady state relative permeability measurement at reservoir condition for both FW and DSSW brines. The key end point saturations and relative permeability values for each plug/experiment are summarized in Table 5. The analytical lab data and corresponding simulated data by Sendra are shown through Figures 7-12, where a good history matched production profiles, differential pressures and water saturation profiles are observed on the left. The simulated relative permeability curves by LET correlations [15] are also illustrated in linear-linear and semi-log format on the right, respectively.

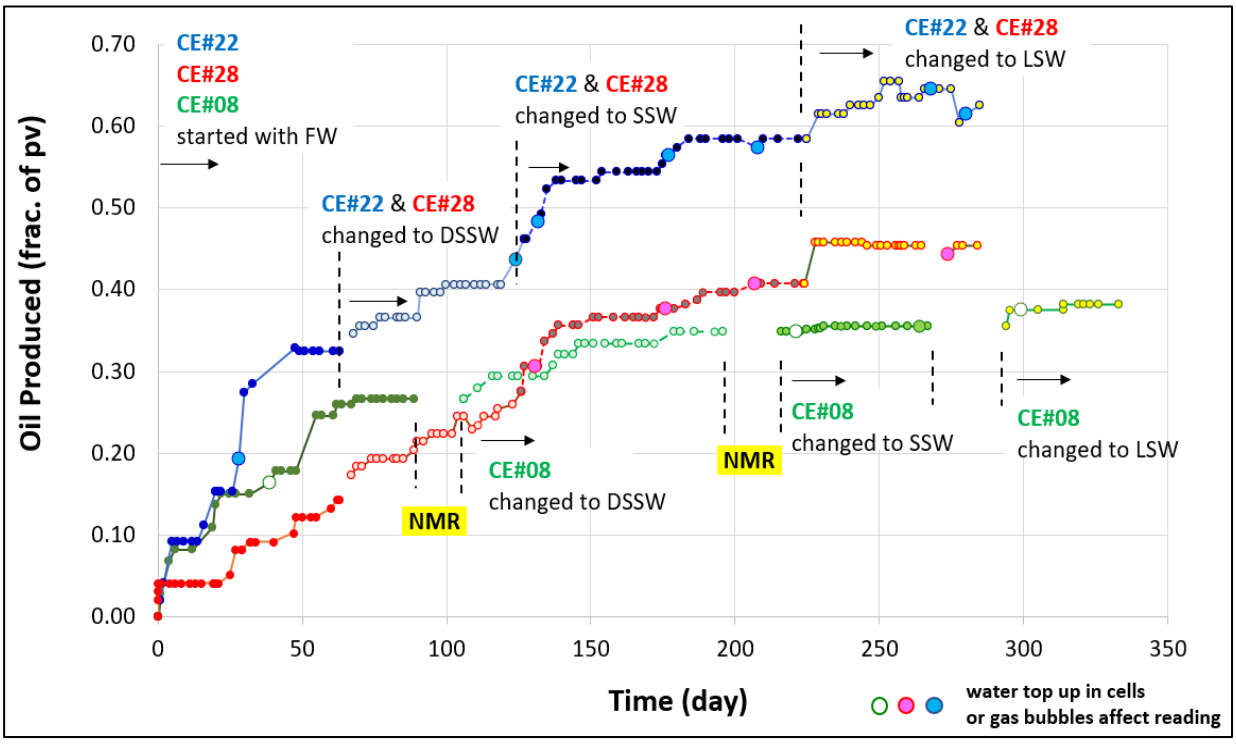

Fig. 6. Effect of different brine on oil recovery over time (as fraction of pore-volume, pv) for each core plug tested.

Table 5. Experimental and simulated endpoints values

	S_{wi}[1] (frac.)		K_o@S_{wi}[1] (mD)		S_{orw}[2] (frac.)		K_{rw}@S_{orw}[2] (frac.)	
Brine / Plug#	FW	DSSW	FW	DSSW	FW	DSSW	FW	DSSW
1	0.141	0.137	109.3	149.6	0.17	0.24	0.55	0.65
2	0.268	0.297	13.4	20.6	0.10	0.125	1.00	0.70
3	0.179	0.297	518	555	0.375	0.1	0.21	0.50

1: Measured
2: Simulated by Sendra history matching (more reliable)

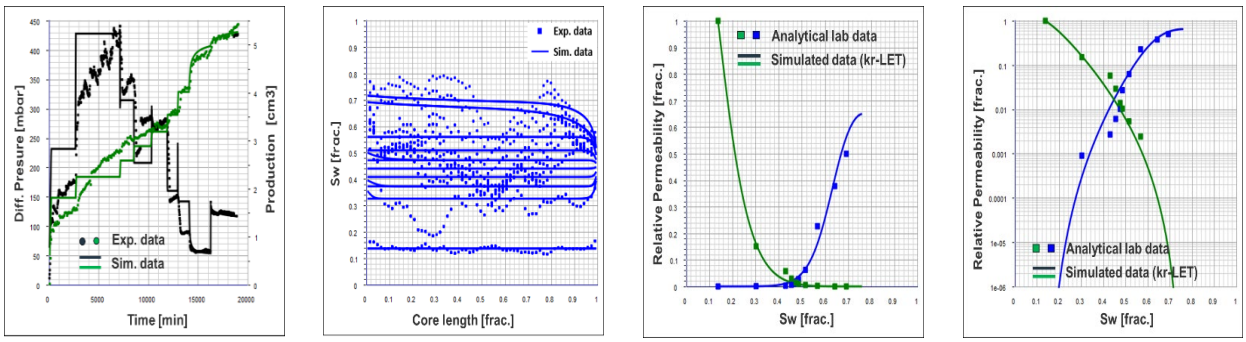

Fig. 7. Plug#1-Oil/DSSW system: Experimental and simulated differential pressure, production, and saturation profile of the steady state experiment are shown on the left. The simulated (i.e. history matched) relative permeability by LET correlations are shown together with analytical data in linear-linear and semi-log format on the right.

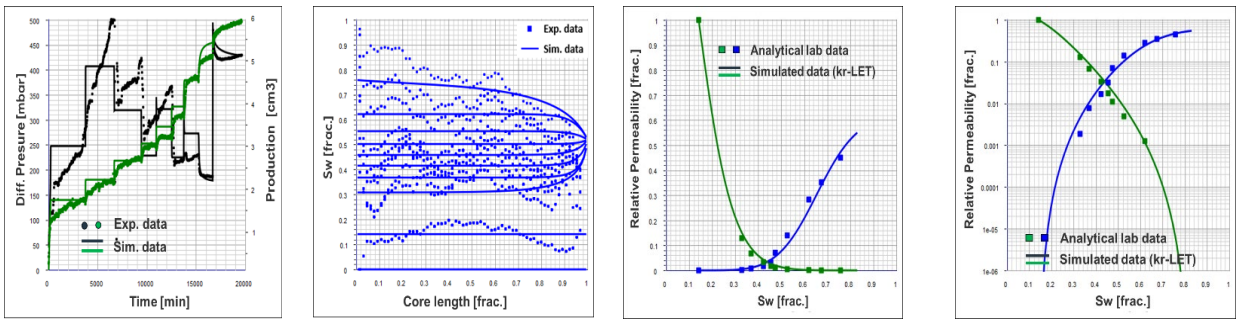

Fig. 8. Plug#1-Oil/FW system: Experimental and simulated differential pressure, production, and saturation profile of the steady state experiment are shown on the left. The simulated (i.e. history matched) relative permeability by LET correlations are shown together with analytical data in linear-linear and semi-log format on the right.

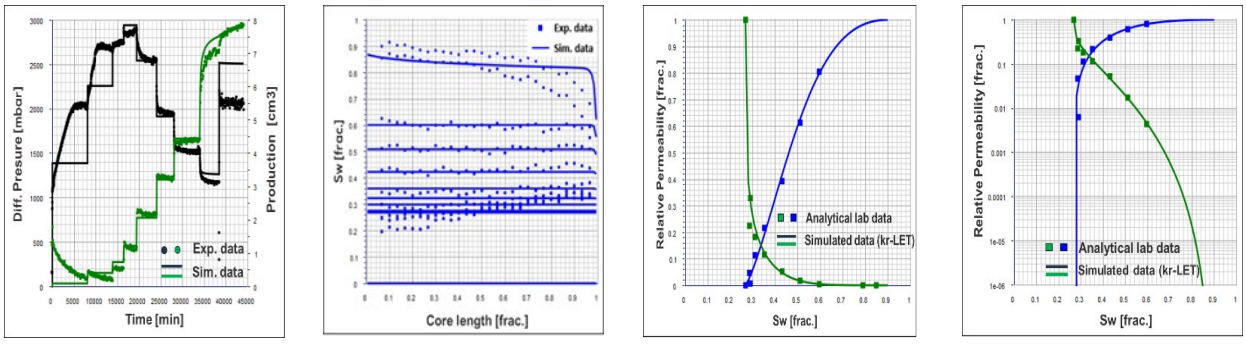

Fig. 9. Plug#2-Oil/FW system: Experimental and simulated differential pressure, production, and saturation profile of the steady state experiment are shown on the left. The simulated (i.e. history matched) relative permeability by LET correlations are shown together with analytical data in linear-linear and semi-log format on the right.

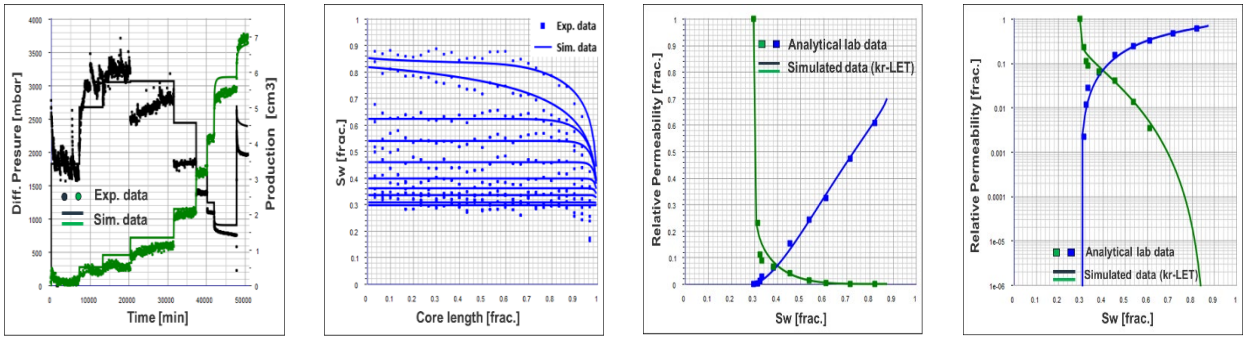

Fig. 10. Plug#2-Oil/DSSW system: Experimental and simulated differential pressure, production, and saturation profile of the steady state experiment are shown on the left. The simulated (i.e. history matched) relative permeability by LET correlations are shown together with analytical data in linear-linear and semi-log format on the right.

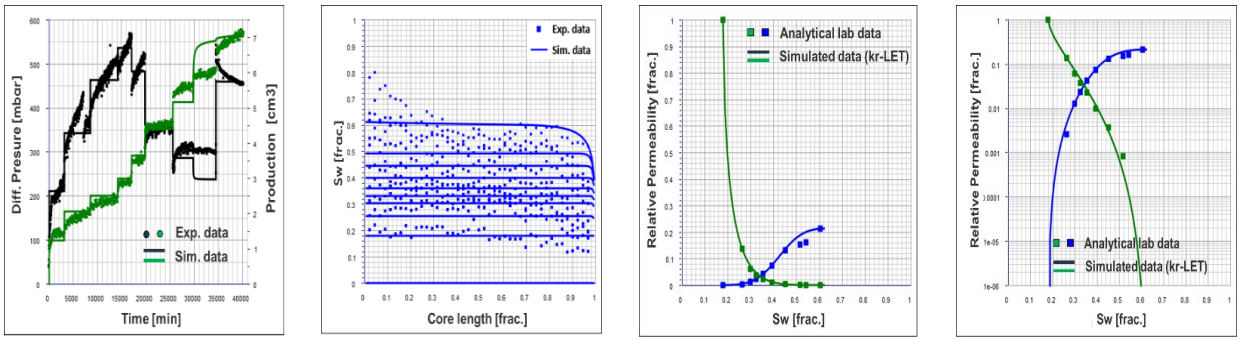

Fig. 11. Plug#3-Oil/FW system: Experimental and simulated differential pressure, production, and saturation profile of the steady state experiment are shown on the left. The simulated (i.e. history matched) relative permeability by LET correlations are shown together with analytical data in linear-linear and semi-log format on the right.

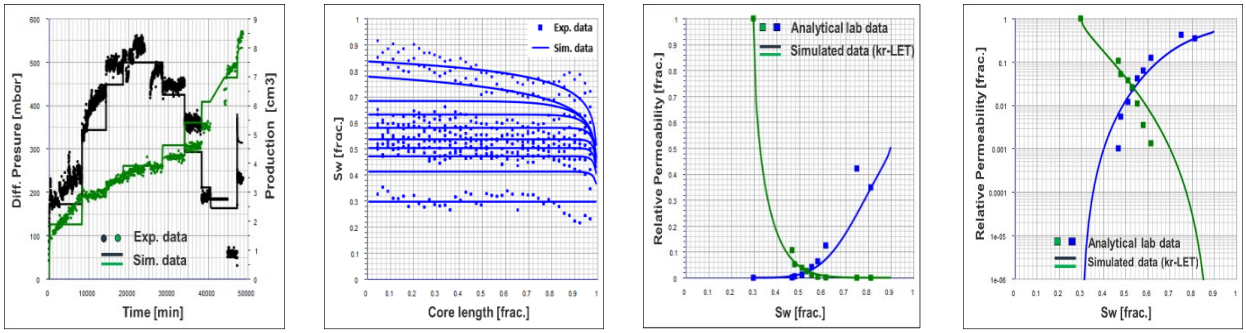

Fig. 12. Plug#3-Oil/DSSW system: Experimental and simulated differential pressure, production, and saturation profile of the steady state experiment are shown on the left. The simulated (i.e. history matched) relative permeability by LET correlations are shown together with analytical data in linear-linear and semi-log format on the right.

Plug#1 undergone steady state study first by DSSW and then followed by FW, whereas the other 2 core plugs, the experiments were performed first with FW followed by DSSW. The comparison between the normalized relative permeability curves for both oil/FW and oil/DSSW system on all 3 plugs are given in the Figures 13-15 both in linear-linear and semi-log format as well as the comparison between corresponding fractional flow (F_w) for both fluid systems. The solid line represents oil/DSSW experiments, and dashed line is for oil/FW cases.

At the first glance, it can be observed that there is almost no difference oil relative permeability behaviour for all three plugs on the path towards S_{orw}, where no clear conclusions can be withdrawn with respect to potential decrease in S_{orw} due to wettability alteration caused by DSSW.

But, on the other hand, a clear shift of the relative permeability sets towards right can be observed for plug#2 and plug#3, particularly on the cross-point of K_{ro} and K_{rw} curves that supports the wettability alteration towards a less oil-wet condition (i.e. increased water wetness) following Craig criteria to determine wettability [17]. For plug#1, it is also interesting to see that despite the fact that it has undergone steady state study first by DSSW and then followed by FW, the corresponding crossing point for oil/FW relative permeability curves is located on the left compared to the crossing point of oil/DSSW system, which is also in line with Craig criteria indicating more water-wet behaviour as illustrated in Figure 13.

The shift towards right is also evident in F_w curves for plug#2 and #3 as also shown in Figure 14 and Figure 15, respectively that indicates later breakthrough for

oil/DSSW system. The contrary behaviour of F_w for plug#1 under oil/FW system, is separately discussed later in this section.

As the Craig's third rule [17], a reduction of the end-point relative permeability to water at residual oil saturation ($K_{rw}@S_{orw}$) is also considered as wettability changes to a more water-wet condition. In this study, the only core plug that presented such response was plug#2 as shown in Figure 14 with a noticeable reduction in $K_{rw}@S_{orw}$ (i.e. from 1 to 0.7)), which is more evident than other two plugs in oil/DSSW system compared to oil/FW system.

For plug#1, $K_{rw}@S_{orw}$ and S_{orw} for oil/FW compared to oil/DSSW system, are reduced from 0.65 to 0.55 and 0.24 to 0.17, respectively, which are in contrary to Craig criteria for increased water wetness of the rock as expected for oil/DSSW system. Both reduction in $K_{rw}@S_{orw}$ and S_{orw} as well as the advancement of F_w towards right for oil/FW system, may be anticipated that wettability alteration of pore surfaces has already been made by the prior oil/DSSW SS-kr experiments, where the aging process in the second run (oil/FW system) might not have been able to re-establish the original wetting state. In other words, plug#1 has undergone oil/FW Kr study with less oil-wet condition compared to oil/DSSW study.

Alzubaidi et al [18] showed a clear shift to the right of oil/water relative permeability curves for water-wet system compared to mixed-wet system. Adityawarman et al [19] also captured wettability alteration by LSW using shifted relative permeability curves under field application study as an EOR method.

For plug#3, the relative permeability data comparison becomes less reliable since there is more than 10-saturation points difference between two established initial water saturation (0.179 for FW and 0.297 for DSSW) as given in Table 5, in which they should be essentially almost the same regardless of the type of brine in experiment. This difference was anticipated to be due to uncertainty in lab under S_{wi} re-establishment for the second experimental run (i.e. oil/DSSW). But, It is worth to be mentioned that for plug#3 data as shown in Figure 15, in case the relative permeability sets for both oil/FW and oil/DSSW systems are normalized to S_{wi}, it demonstrates evidences for wettability alteration of the rocks using desulphated sea water, where a decrease in S_{orw} and right-shift of relative permeability and fractional flow for oil/DSSW system is clearly exhibited.

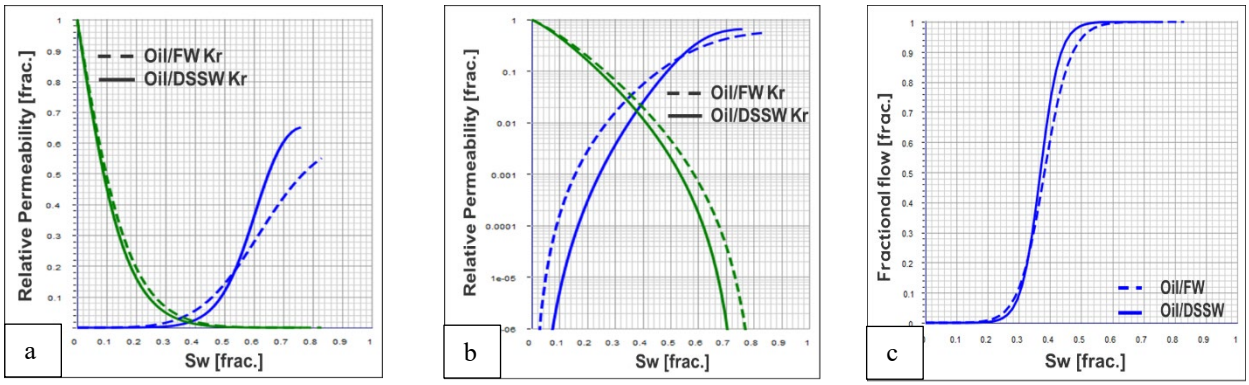

Fig. 13. Plug#1: Comparison between LET simulated relative permeability curves in normalized version to S_{wi} for Oil/FW (dashed line) and Oil/DSSW (solid line) showing in a) linear-linear format, b) semi-log format and c) corresponding fraction flows: water in blue and oil in green.

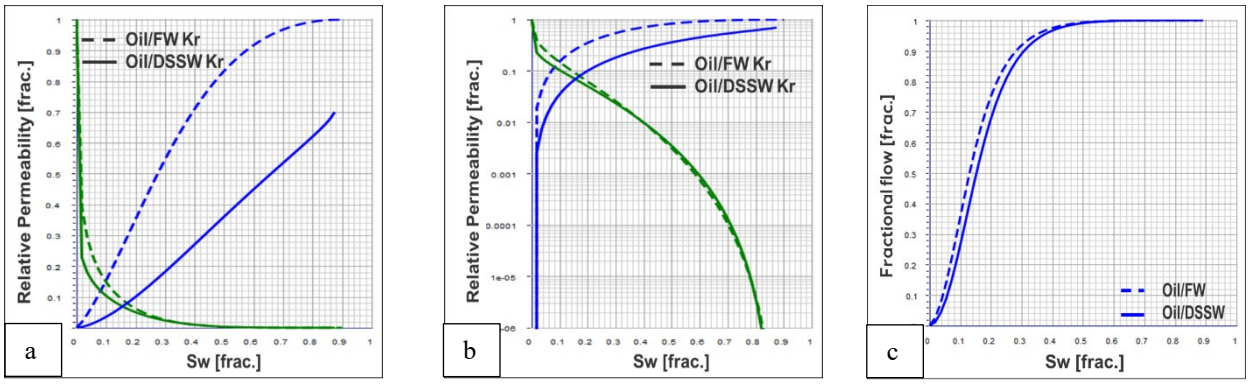

Fig. 14. Plug#2: Comparison between LET simulated relative permeability curves in normalized version to S_{wi} for Oil/FW (dashed line) and Oil/DSSW (solid line) showing in a) linear-linear format, b) semi-log format and c) corresponding fraction flows: water in blue and oil in green.

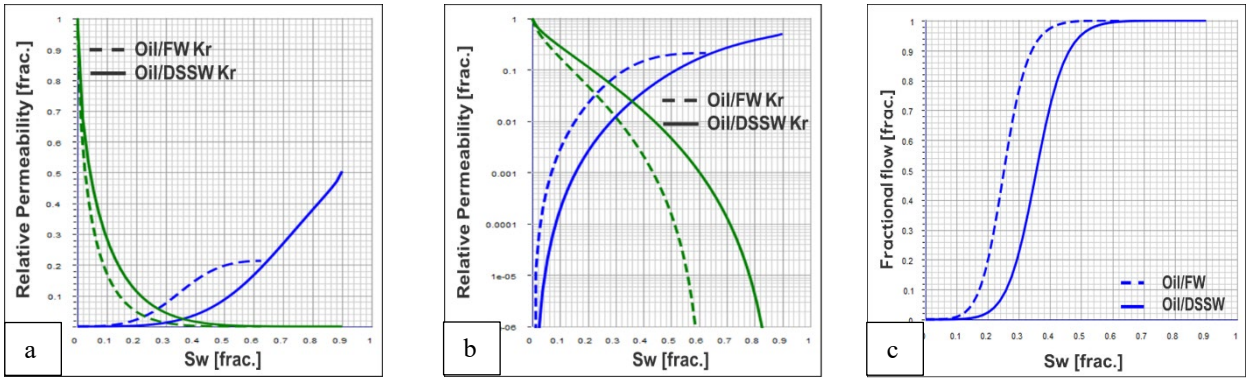

Fig. 15. Plug#3: Comparison between LET simulated relative permeability curves in normalized version to Swi for Oil/FW (dashed line) and Oil/DSSW (solid line) showing in a) linear-linear format and b) semi-log format c) corresponding fraction flows: water in blue and oil in green.

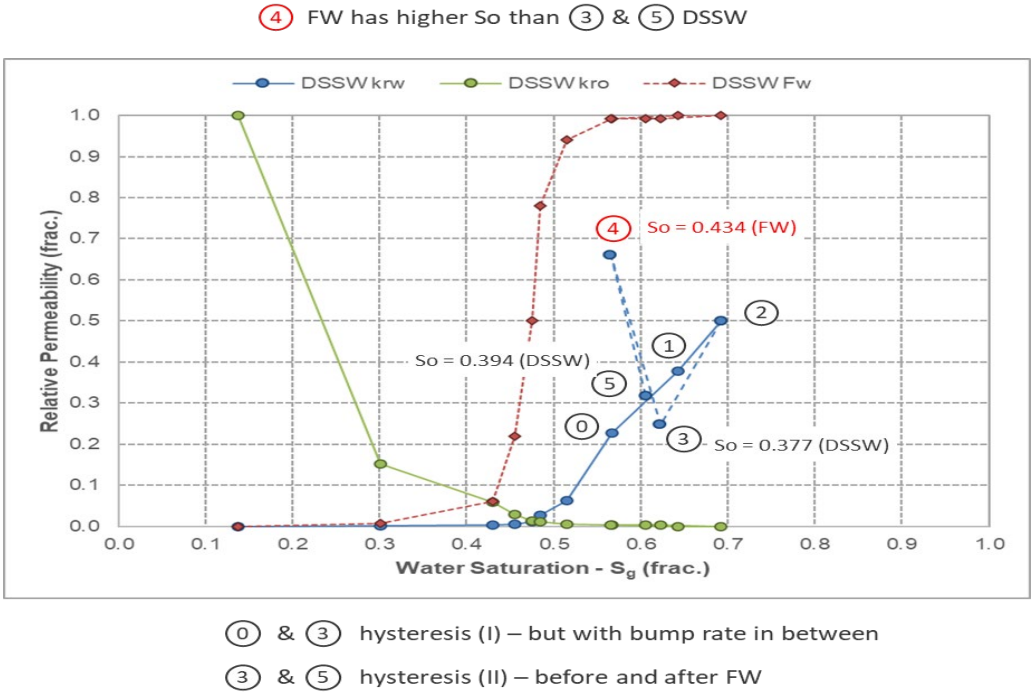

Fig. 16. Dynamic response of water saturation to salinity.

To further investigate wettability alteration effects of brine salinity on plug#1, additional experimental procedures were performed at the end of standard SS cycle (i.e. after bump rate stage with DSSW at 100% water cut as point 2 shown in Figure 16 and Table 6. Firstly, oil was reintroduced into the core together with DSSW and at a water cut (i.e. F_w) of 0.992, as point 3 in Figure 16. Secondly, when steady state reached and whilst keeping both the flow rate and water cut constant the injected brine was switched from DSSW to FW, point 4 in Figure 16. Finally, upon reaching steady state the injected brine was switched from FW back to DSSW again, point 5 in Figure 16. The change in saturations due to these brine switches are shown in Table 6 where a 4-6% increase in oil recovery in favour of the lower saline DSSW can be seen. Furthermore, the changes in water saturation with the brine salinity appears to be reversible. The proximity between points 3 and 5 in Figure 16 indicates that there was minimal hysteresis during these switches. This complementary study illustrates the dynamic response of the wettability due to changes in the brine salinity.

Table 6: Saturation changes during dynamic brine switch

	Plug#1 - DSSW			
step	F_w (frac.)	injected brine	S_w (frac.)	(DSSW-FW) Δ Sw
0	0.992	DSSW	0.567	
1	1.000	DSSW	0.643	
2	bump 1.0	DSSW	0.693	
3	0.992	DSSW	0.623	
4	0.992	FW	0.566	0.057
5	0.992	DSSW	0.606	0.041

3.3 Reservoir simulation results

In addition to the numerical core flood simulations done on plug scale by Sendra software, it was also attempted to perform some reservoir simulation study in at field scale model by Eclipse 100™ [20], where the main findings from the laboratory tests were employed as input. It follows the safe approach of performing oil recovery estimates based on experimental data.

When it comes to field scale model, two types of models have been considered: sector model and full field model. The objective of using different field scales was to capture the effects low salinity brine injection considering the following aspects: sophistication level of low salt implementation in the models and oil recovery estimates in both well and field level. Both models use black-oil and single porosity formulation but considering different well counts and dynamic constraints.

3.3.1 Sector model

A sector model (3 km x 1.5 km and around 115000 cells) based on dip direction of the full field model including three wells has been built. The wells considered are one gas injector at crest, one oil producer at mid-flank and one down-flank water injector as shown in Figure 17.

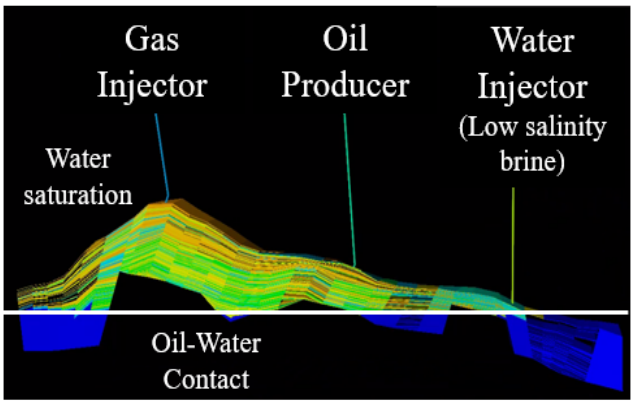

Fig. 17. Sector model showing a dip cross section and wells location on initial water saturation distribution map.

To ensure that the sector model reproducing main full field dynamic responses, proper boundaries were created considering increased pore volume on close by active cells. Wells have been completed considering reasonable distance between producer and injectors both in lateral and vertical direction. The water injection well starts after a couple of years when the reservoir is depleted easing the injection of reduced salt water.

The low salt implementation in simulation models was done using the keyword LOWSAL in Eclipse 100™ assuming a reduction in residual oil saturation (S_{orw}) of 5% for low salinity relative permeability curves. By the time of running sector model simulation study, the SCAL data was only available for plug#1 oil/DSSW system, hence the assumption made here, is based on the average value of plug#1 tested during the SS-K_r test ("switch brine" stage) as discussed in the previous section, Table 6 and Figure 16. $K_{rw}@S_{orw}$ values were defined in terms of two wettability scenarios based on limited data available in our internal SCAL database with large uncertainty and prior to all SCAL data are in place. Hence, the corresponding $K_{rw}@S_{orw}$ for formation water (high salinity) and injection water (low salinity) were defined as 0.38 and 0.21, respectively, representing formation water as more oil-wet and injection water as more water-wet (or less oil-wet).

One important aspect of this implementation is that relative permeability curves for high and low salinity are interpolated for mixed concentrations according to defined transition functions, i.e., the weight of each set of relative permeability curves as a function of brine concentration. The brine concentration threshold for starting the low salinity effect was considered as approx. 100k ppm. Using this approach both static and dynamic effect of low salinity brines are included in simulations. In terms of oil recovery gain simulations indicate an increase of up to 2% in cumulative production depending on transition definition (Figure 18). One reason for this relatively small increment is the fact that this specific field has its drainage strategy mainly based on gas injection resulting in a second order mechanism of the water flooding. Noted also that the mixing of injected water with in-situ water delays the attainment of low salinity effects.

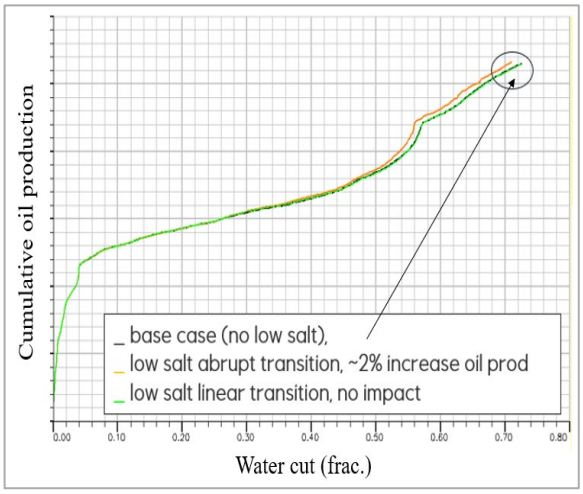

Fig. 18. Cumulative oil production vs. water-cut for low salt effects using different transition functions.

3.3.2 Full Field model

For the full field dynamic simulation, it was used a black oil model with around six million cells. A cross-section of full field model is shown in Figure 19. In order to get quicker simulation results, it was decided to test the model without LOWSAL option and just using simplified approach for oil-water flow given that the main drive mechanism in the field is gas injection. This decision was justified since the model was very large and CPU-demanding in which low salt option would increase even more running time. The simplified approach also allows oil recovery estimate in a context of "high case/optimistic scenario" given instantaneous wettability change effects that can be further investigated in case of

significative variation on production was observed. So, in short, only one single geological realization was tested with two sets of relative permeability tables, i.e. one simulation case for oil/FW system and another one with oil/DSSW system for the main reservoir rock type while other rock types were also defined with their own allocated relative permeability contributing to the fluid flow.

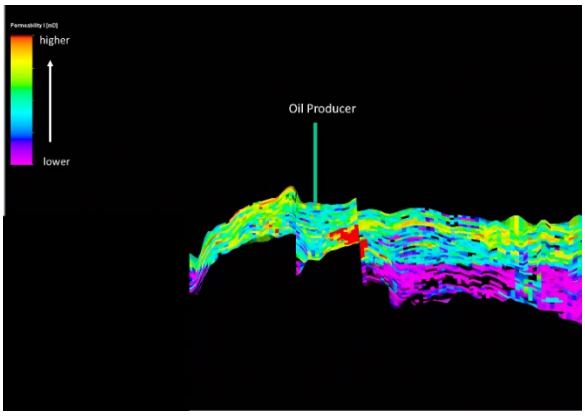

Fig. 19. Full field model showing a vertical cross section on permeability distribution map and a selected well location.

The relative permeability data for plug#2 shown in Figure 14 were selected as input to full field reservoir simulation model to compare the oil and water production performance behaviour mainly at field level and one selected well as shown in Figure 19. The simulation results are shown in Figure 20 and Figure 21 for cumulative oil and water production at field and well level, respectively. It is clearly revealed that almost no or slightly differences are observed for the cumulative oil production at field level (green solid and dashed lines) due the fact that there is almost no difference in oil relative permeability used from SS study for both oil/FW and oil/DSSW systems. It can also be explained based on the reservoir heterogeneity role (co-existence of other rock types and corresponding relative permeability sets in the model) and the constrains in the oil/water production due to limited gas processing capacity that will impact the total cumulative oil production at field level. But, interestingly for a selected well marked as oil producer in Figure 19, the cumulative oil production is higher in case oil/DSSW system compared to oil/FW system as shown in Figure 21. Unlike the minor additional oil recovery at field level, the increased cumulative oil production for the selected oil producers is indicating the effects of wettability change on displacing oil by injected water in some regions of the reservoir.

It is also seen that the cumulative water production at both field and well level is reduced using DSSW relative permeability (blue solid lines in Figures 20-21), which can be interpreted as improved oil recovery, where less water is produced. Mahmoodi et al. [11] similarly used a set of relative permeability curves obtained from core flooding experiments in a sector model for simulation. They also concluded an enhancement in oil recovery while the water-cut is reduced using desulphated brine relative permeability.

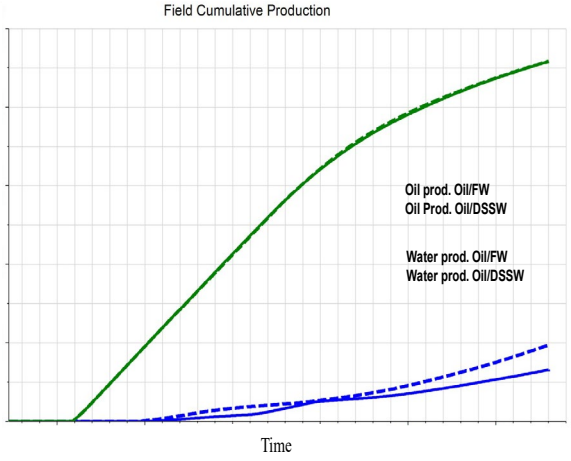

Fig. 20. Field cumulative oil and water production using Oil/FW (dashed line) and Oil/DSSW relative permeability data (solid line). Oil production rate is in green and water production rate is in blue.

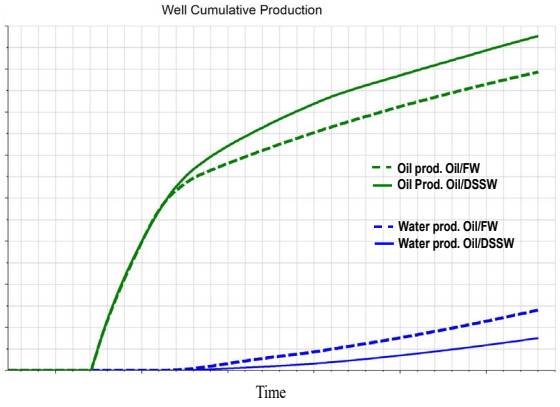

Fig. 21. Well cumulative oil and water production using Oil/FW (dashed line) and Oil/DSSW relative permeability data (solid line). Oil production rate is in green and water production rate is in blue.

Conclusion

Both spontaneous imbibition and relative permeability tests showed that, there are clear evidences of salinity impacting on matrix wettability that lead to changes in water saturations (i.e. wettability alteration) for mixed to oil-wet pre-salt carbonates. It was also observed that such processes are shown to be reversible and responsive to the rate of changing salinity.

The reservoir simulation results from sector model using LOWSAL option, S_{orw} and $K_{rw}@S_{orw}$ from experimental lab data, showed an increased in cumulative oil production by 2%, whereas in full field model, almost no improvement in the oil production rate was observed since there was almost no difference in oil relative permeability for both oil/FW and oil/DSSW systems. But in contrast to oil relative permeability and

field oil production behavior, a reduction in $K_{rw}@S_{orw}$ as well as changes in whole water relative permeability curves for DSSW compared to FW clearly led to a considerable reduction in water production rate (i.e. later break through and lower water cut) that can be interpreted as IOR mechanism for the pre-salt carbonate reservoir.

This study was performed just on one rock type but as a further work in future, it is worth and interesting to perform more similar investigation on other rock types that exist in pre-salt carbonates.

Acknowledgements

The authors would like to thank Equinor ASA, Equinor Brazil and partners for giving permission to publish the data. Also, especial thanks to Equinor SCAL specialist Einar Ebeltoft for valuable discussions and QC of Sendra simulation part of this study.

Nomenclature

DSSW: Desulphated Synthetic Sea Water
F_w: fractional flow
FW: Formation Water
$K_o@S_{wi}$: Absolute permeability to oil at S_{wi} as base permeability
$K_{rw}@S_{orw}$: Endpoint relative permeability to water at residual oil saturation
LSW: Low salinity (Sea) Water
S_{orw}: Residual oil saturation
SSW: Synthetic Sea Water
S_{wi}: Initial water saturation

References

1. A. Katende, F. Sagala, J. Molecular Liquids, **278**, 627-649 (2019).
2. Petrowiki: Low-salinity water flooding (spe.org)
3. G.G. Bernard, SPE 1725 (1967).
4. S.B. Nande, S.D. Patwardhan, J. Petrol. Exp. and Prod. Tech., **12,** 1037–1055 (2022).
5. M.H. Derkani, A.J. Fletcher, W. Abdallah, B. Sauerer, J. Anderson, Z.J. Zhang, Colloids Interfaces, **2**, 20 (2018).
6. J. Hao, S. Mohammadkhani, H. Shahverdi, M. Nasr Esfahany, A. Shapiroc, J. Petrol. Sci. and Eng., **179**, 276–291(2019).
7. R. Mokhtari, S. Ayatollahi, M. Fatemi, J. Petrol. Sci. and Eng., **182**, 106194 (2019).
8. P. Rostami, M. F. Mehraban, M. Sharifi, M. Dejam, S. Ayatollahi, Petroleum, **5,** 367–374 (2019).
9. H. Mahani, A. L. Keya, S. Berg, W-Bart Bartels, R. Nasralla, W. R. Rossen, Energy Fuels, **29,** 1352−1367 (2015).
10. X. Wang, W. Liu, L. Shi, Z. Zou, Z. Ye, H. Wang, L. Han, J. Petrol. Sci. and Eng., **207**, 109153 (2021).
11. A. Mahmoodi, S.B. Hosseinzadehsadati, H.M. Kermani, H.M. Nick, Science of the Total Environment, **904,** 166732 (2023).
12. F. Bordeaux-Rego, J. A. Ferreira, C. A. S. Tejerina, K. Sepehrnoori, Energies, **14,** 3043 (2021).
13. A. C. L. Sartorato, S. N. Tonietto, E. Pereira, Rio Oil & Gas Expo and Conference, ISSN 2525-7579, (2020).
14. Sendra User guide 2020.1, PRORES AS, (2020)
15. F. Lomeland, E. Ebeltoft, W.H. Thomas, paper SCA 2005-32, presented at the International Symposium of the Society of Core Analysts, Toronto, Canada (2005).
16. T. Ramstad, A. Kristoffersen, L. Rennan, R. Wat, C.J.T. De Lima, presented at Second EAGE Conference on Pre-Salt Reservoir, pp.1-5 (2021).
17. F.F. Craig, *SPE Monograph Series* **vol. 3,** Richardson, TX; ISBN:978-0-89520-202-4 (1971).
18. F. Alzubaidi, J. E. McClure, H. Pedersen, A. Hansen, C. F. Berg, P. Mostaghimi, R. T. Armstrong, arXiv:2309.00362, **v1** [physics.flu-dyn], A preprint (2023).
19. A. Adityawarman, F. A. Aziz, P. Abdul Aziz, P. Yusgiantoro, S. Chandra, J. Earth Energy Eng. **vol. 9,** no. 1, pp 18-36 (2020)
20. ECLIPSE, SLB, product, (2023)